Available online at www.sciencedirect.com
SCIENCE DIRECT®
Journal of Sound and Vibration 280 (2005) 1066–1074
JOURNAL OF SOUND AND VIBRATION
www.elsevier.com/locate/jsvi

Short Communication

Vibration of an axially moving beam wrapping on fixed pulleys

Lingyuan Kong, Robert G. Parker*

Department of Mechanical Engineering, The Ohio State University, Columbus, OH 43210-1107, USA

Received 5 February 2004; accepted 17 February 2004

Available online 18 September 2004

1. Introduction

Systems where an axially moving continuum wraps around rotating pulleys occur in serpentine belt drives, band saws, data storage tape drives, paper handling machinery, thread and fiber winders, and so on. In the literature, axially moving continua have been studied extensively, especially for the belt or band in a single span decoupled from the pulleys. In this case, the belt/band is modeled as a moving string (without bending stiffness) or a moving beam (with bending stiffness) subject to specified boundary conditions. These are the simplest models and are the basis for most axially moving media analysis.

For the axially moving beam model, the span boundary conditions are typically specified as simply supported or clamped, and the beam is assumed to remain straight in the steady state. In most practical systems, however, the beam wraps around two fixed pulleys. This induces initial curvature in the steady state for non-vanishing bending stiffness, and the beam–pulley contact points are not on the common tangent between the pulleys.

Some research considers the effects of the beam wrapping around the pulleys, which influences the steady and dynamic motion of the beam [1–9]. Turnbull et al. [9] study the nonlinear contact effect of belt wrapping and unwrapping during motion by using perturbation methods. Alternatively, one can consider the beam wrapping on the pulley only in calculating the steady state around which the linearized beam motion occurs. For the steady-state solution, the span boundary conditions including the beam wrapping effect are treated in two different ways. The

*Corresponding author. Tel.: +1-614-688-3922; fax: +1-614-292-3163.
E-mail address: parker.242@osu.edu (R.G. Parker).

0022-460X/$ - see front matter
doi:10.1016/j.jsv.2004.02.037

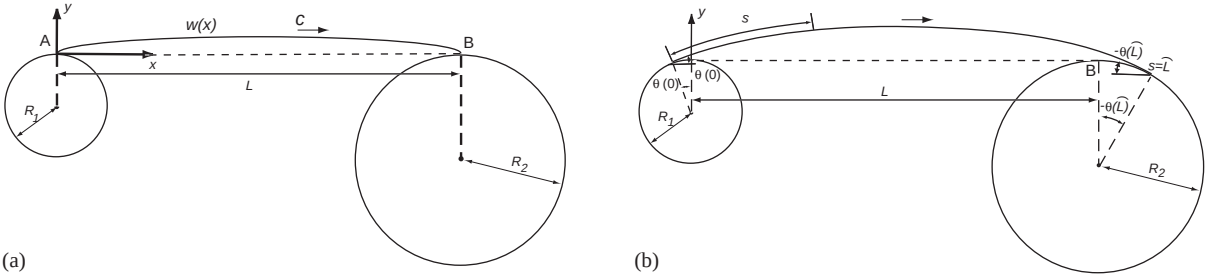

Fig. 1. (a) Fixed boundary model; and (b) undetermined boundary model.

first way (Fig. 1(a)) assumes the beam–pulley contact points are fixed on the common tangent line between the two pulleys. The steady motion analysis uses simple supports with moments of EI/R applied at the boundaries, where EI is the beam bending rigidity and R is the bounding pulley radius. Linear vibration about the steady state can be investigated [4,6–8]. The second boundary condition treatment (Fig. 1(b)) eliminates the restriction that the contact points lie on the common tangent. Instead, the contact points are not specified a priori but are calculated (along with the steady beam deflections and tension distributions) from a steady-state analysis of the beam in the free spans [2,3,5]. Hwang and Perkins [2,3] study the steady state and free vibration of a single beam span stretched between one fixed pulley and a spring-loaded pulley. Kong and Parker [5] consider the steady-state mechanics of a two-span system with two fixed pulleys in which the beam transverse and longitudinal inertia is incorporated.

Of these two different ways of modeling the beam wrapping around the pulleys, the first one is much simpler but sacrifices some model fidelity. No quantitative comparison addressing the impact of these modeling options on the vibration properties has been found in the literature. In this note, the free vibration differences between these two models dealing with the beam–pulley wrapping effect are highlighted for a beam span between two fixed pulleys (the usual case in applications). The results of these two non-trivial steady-state models are compared with the commonly used model of simple supports with a straight (trivial) steady solution. When the bending stiffness is small, the natural frequency differences between these different models are minor, but the differences are pronounced for larger bending stiffness still within the practical range of industrial systems.

2. Fixed boundary model

Fig. 1(a) shows a single span beam stretched between two fixed pulleys. The span admits the transverse displacement $w(x,t)$. The beam moves with constant speed c and has fixed span length L, where the boundary points A and B lie on a line tangent to both pulleys. The span is subject to constant moments at its ends due to wrapping of the beam around the pulleys [4,6–8]. This gives the boundary conditions

$$w(0,t)=0, \quad EI\,w_{,xx}(0,t)=-\frac{EI}{R_1}, \quad w(L,t)=0, \quad EI\,w_{,xx}(L,t)=-\frac{EI}{R_2}. \tag{1}$$

The nonlinear equation of motion is [10]

$$m(w_{,tt} - 2cw_{,xt} + c^2 w_{,xx}) - \left[\left(P_0 + \frac{\mathrm{EA}}{L}\int_0^L \tfrac{1}{2}w_{,x}^2\,\mathrm{d}x\right)w_{,x}\right]_{,x} + \mathrm{EI}\,w_{,xxxx} = 0, \tag{2}$$

where m is the beam mass density per unit length, P_0 is the initial tension, EA is the longitudinal stiffness, and EI is the bending stiffness. The integral term in Eq. (2) comes from the quasi-static stretching assumption that the dynamic tension is a function of time but does not vary along the beam. This is reasonable for most applications where $\mathrm{EA}/P_0 \gg 1$ and longitudinal waves propagate much more rapidly than transverse waves.

From Eq. (2), the steady-state displacement w^* is governed by

$$\mathrm{EI}\,w^*_{,xxxx} - Pw^*_{,xx} = 0, \tag{3}$$

where $P = P_0 - mc^2 + (\mathrm{EA}/L)\int_0^L \frac{1}{2}(w^*_{,x})^2\,\mathrm{d}x$ is the tension in the steady state. The boundary conditions are similar to Eq. (1) except that all w are replaced by w^*.

Linearization of the general dynamic equation (2) about the steady-state configuration $w^*(x)$ yields

$$mw_{,tt} - 2mcw_{,xt} - Pw_{,xx} + \mathrm{EI}\,w_{,xxxx} - \mathrm{EA}\left(\int_0^L w_{,x}w^*_{,x}\,\mathrm{d}x\right)w^*_{,xx} = 0, \quad 0 < x < L, \tag{4}$$

where $w(x,t)$ now represents the small vibration about $w^*(x)$. The homogeneous boundary conditions for $w(x,t)$ are

$$w(0,t) = 0, \quad w_{,xx}(0,t) = 0, \quad w(L,t) = 0, \quad w_{,xx}(L,t) = 0. \tag{5}$$

Galerkin discretization of Eqs. (4) and (5) is readily applied to find the natural frequencies and vibration modes. The chosen basis functions are $\psi_n(x) = \sin(n\pi x/L), \quad n = 1,2,3\ldots$

This model includes steady beam deflection $w^*(x)$ in the formulation but allows no deviation of the boundary points caused by beam wrapping. This creates slope discontinuities (or kinks) at A and B (Fig. 1(a)). A simpler model, which is the one most commonly used, results from ignoring steady beam deflection with $w^*(x) = 0$ in Eqs. (4) and (5).

3. Undetermined boundary model

Instead of specifying the boundaries for the beam span at the points of common tangency, the boundaries of the span in the steady state can be determined by the geometric conditions that: (a) the beam end curvature equals the inverse of the end pulley radius, and (b) the curved beam contacts and is tangent to the end pulleys. The boundaries are unknown a priori (Fig. 1(b)). This model eliminates the slope discontinuity at the span boundaries. With this model, the steady-state governing equations for the moving beam in a free span are [5]

$$(\hat{P} - GV)' + EI\kappa\kappa' = 0, \quad (\hat{P} - GV)\kappa - EI\kappa'' = 0, \tag{6}$$

where $\hat{P}(s)$ and $V(s)$ are the beam tension and speed along the beam, G is the constant mass flow rate, $\kappa = \mathrm{d}\theta/\mathrm{d}s$ is the beam curvature, θ is the inclination angle measured from the due east direction, and $'$ represents differentiation with respect to the arc coordinate s (Fig. 1(b)). Notice

beam inertia is included in Eq. (6) in the longitudinal and transverse (centripetal acceleration) directions. The constitutive law $\bar{P} = \mathrm{EA}(m_0 V/G - 1)$ links the field variables $\bar{P}(s)$ and $V(s)$, where m_0 is the mass density per unit length in the stress-free state [5,11–13]. The total arclength $\bar{L}$ is not known a priori; it is determined from the requirement that the curved beam contacts and is tangent to both bounding pulleys. This steady system can be mathematically reformulated to a standard form with two fixed boundaries and numerically exact steady-state solutions are calculable [5].

Linearized motion about the steady solution $\hat{w}^*(x)$ for the undetermined boundary model is governed by

$$mw_{,tt} - 2mcw_{,xt} - Pw_{,xx} + \mathrm{EI}\, w_{,xxx} - \mathrm{EA}\left(\int_0^{\bar{L}} w_{,x}\hat{w}^*_{,x}\,\mathrm{d}x\right)\hat{w}^*_{,xx} = 0. \tag{7}$$

The distinctions between Eqs. (7) and (4) are that: (a) w^* is replaced by $\hat{w}^*$, which represents the steady state of the undetermined boundary model, and (b) $\bar{L}$ is the straight distance between the two boundary points in Fig. 1(b), which is longer than L in Fig. 1(a) due to the unwrapping of the beam on the pulleys. Galerkin discretization with the basis functions $\psi_n(x) = \sin(n\pi x/\bar{L})$, $n = 1, 2, 3\ldots$ yields the eigensolutions.

In deriving the steady state $w^*(x)$ used in Eq. (4), the tension and speed are uniform throughout the beam. In calculating the steady state in the undetermined boundary model, the tension and speed vary along the beam [5]. To compare results from Eqs. (4) and (7), the speed c and tension P at the span midpoint are applied throughout the beam in Eq. (7).

4. Comparison and discussion

The natural frequencies from the above models are compared in this section. The case where no wrapping is considered (that is, Eqs. (4) and (5) with $w^*(x) = 0$) is referred to as the *trivial equilibrium* case. The beam tension and speed are the same in the free vibration analysis for the three different models, but the steady-state deflections of the free span are different.

The numerical results are presented in dimensionless form. For accurate comparison, the three models are non-dimensionalized in the same way using

$$\hat{x} = \frac{x}{L}, \quad \hat{w} = \frac{w}{L}, \quad \hat{t} = t\sqrt{\frac{P}{mL^2}}, \quad \varepsilon^2 = \frac{\mathrm{EI}}{PL^2}, \quad \hat{v} = c\sqrt{\frac{m}{P}}, \quad \gamma = \frac{\mathrm{EA}}{P}. \tag{8}$$

Substitution of Eq. (8) into Eq. (4) leads to the dimensionless equation for the fixed boundary model (after dropping the hat)

$$w_{tt} + 2vw_{xt} - (1 - v^2)w_{xx} + \varepsilon^2 w_{xxxx} - \gamma\left(\int_0^1 w_{,x}w^*_{,x}\,\mathrm{d}x\right)w^*_{,xx} = 0, \quad 0 < x < 1. \tag{9}$$

The dimensionless form of Eq. (7) is similar to Eq. (9) except $w^*(x)$ is replaced by $\hat{w}^*(x)$ and the limit of integration and right boundary occur at $\bar{L}/L$. The nominal case from which parameter variations are considered is $\varepsilon = 0.06$, $v = 0.5$, $\gamma = 1200$, and $R/L = 1/\pi$. The two end pulleys are assumed to have the same radius R for simplicity.

The steady motions from the three models are shown for varying ε in Fig. 2. The curvature caused by the beam bending around the pulleys increases with bending stiffness. For large bending stiffness, the differences of these three steady states are apparent. The fixed and undetermined boundary models have similar peak-to-peak amplitudes, but the undetermined boundary model has a noticeably longer span length.

Fig. 3 shows the relationship between the natural frequencies and beam bending stiffness. When the bending stiffness is small, the natural frequencies of the fixed boundary model and those of the trivial equilibrium model are very close to each other, but both are higher than the corresponding natural frequencies of the undetermined boundary model. Especially for the third and higher

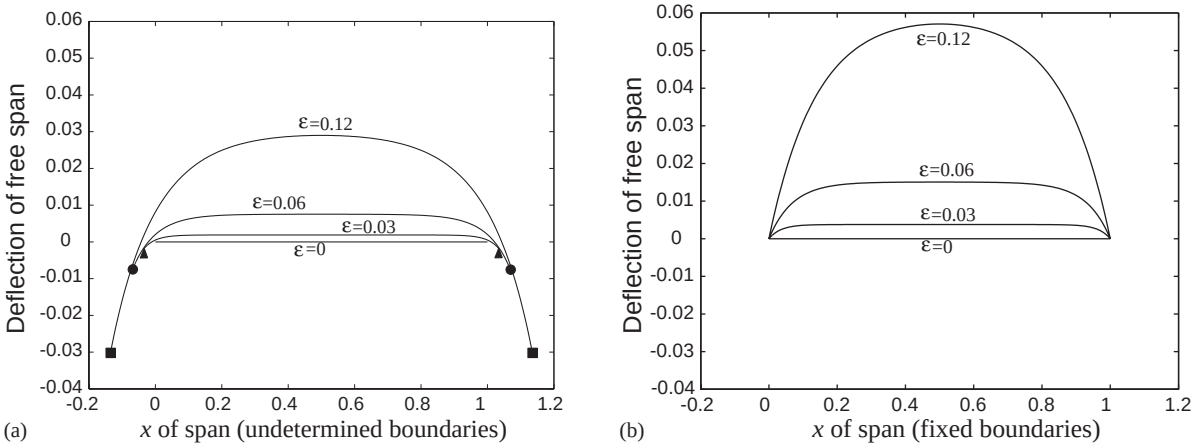

Fig. 2. Comparison of steady states for different models; $v = 0.5$, $R/L = 1/\pi$, $\gamma = 1200$. (a) Undetermined boundary model; and (b) fixed boundary model. $\varepsilon = 0$ corresponds to the trivial equilibrium model.

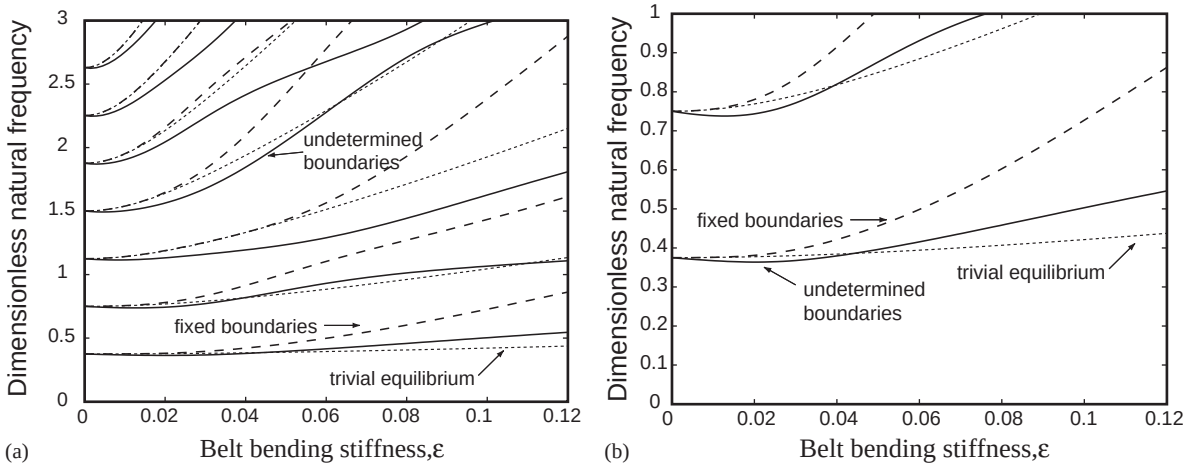

Fig. 3. Dimensionless natural frequencies for varying bending stiffness; $v = 0.5$, $R/L = 1/\pi$, $\gamma = 1200$: (– – –) fixed boundary model; (—) undetermined boundary model; and (···) trivial equilibrium model.

natural frequencies, the differences are clearly evident even for very small ε. For the undetermined boundary model, as bending stiffness increases from zero, the fundamental natural frequency initially decreases in the range $0<\varepsilon<0.0195$, and then increases for bending stiffness larger than 0.0195 (Fig. 3(b)). The second natural frequency behaves similarly. This unusual phenomenon is because there are three different mechanisms that affect the system: (a) bending stiffness increases the free span length, which softens the system, (b) bending stiffness increases the curvature, which stiffens the system, and (c) higher bending stiffness directly increases natural frequencies. The impact of each effect can be assessed by comparing the three models. All three mechanisms are active for the undetermined boundary model. Only the last two are effective for the fixed boundary model. The trivial equilibrium model is affected only by the last mechanism. When bending stiffness is small, the dominant effect is span lengthening for the undetermined boundary model. The increased span length mechanism has no effect on the fixed boundary model, so its natural frequencies are always higher than those of the other two models.

The relationship between the natural frequencies and beam speed is shown in Fig. 4. Natural frequencies do not decrease monotonically with beam speed for both of the non-trivial steady-state models. This differs from the trivial equilibrium model where increasing beam speed monotonically decreases all natural frequencies. Like with bending stiffness, increasing beam speed changes the steady state (Fig. 5) around which free vibration occurs, introducing curvature that stiffens the system. The upward natural frequency shift from increased curvature is mitigated somewhat in the undetermined boundary model because of the increased free span length. Curve veering is apparent in the eigenvalue loci for the non-trivial steady-state models [14].

Fig. 6 shows the effect of end pulley radius on the natural frequencies. For the trivial equilibrium model, pulley radius has no influence on the spectrum of the moving beam, as expected. For the other two models, the natural frequencies decrease as the pulley radius

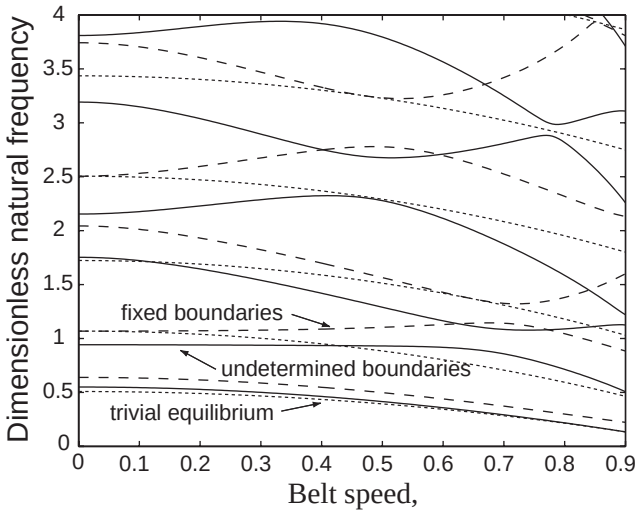

Fig. 4. Dimensionless natural frequencies for varying beam speed; $\varepsilon = 0.06$, $R/L = 1/\pi$, $\gamma = 1200$: (– – –) fixed boundary model; (—) undetermined boundary model; and (···) trivial equilibrium model.

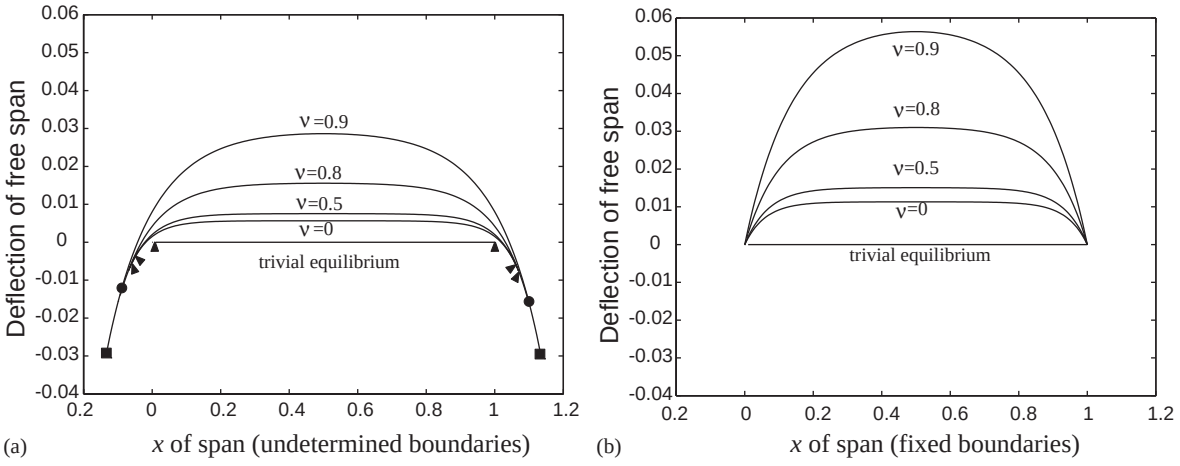

Fig. 5. Steady states for varying beam speed; $\varepsilon = 0.06$, $R/L = 1/\pi$, $\gamma = 1200$. (a) Undetermined boundary model; and (b) fixed boundary model.

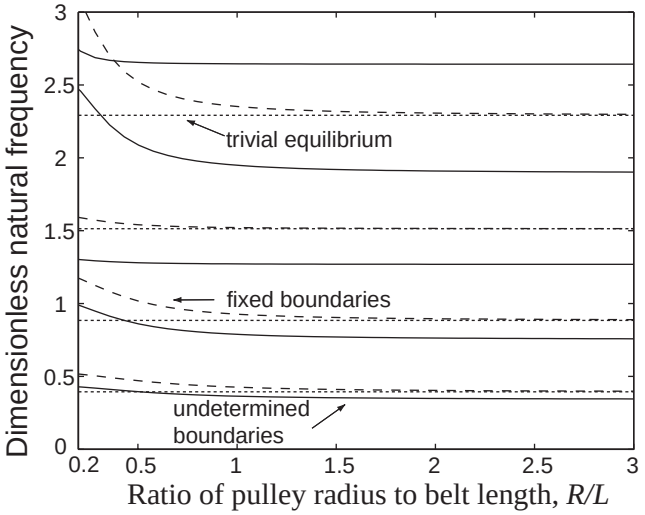

Fig. 6. Dimensionless fundamental natural frequency for varying ratio of pulley radius to beam length; $v = 0.5$, $\varepsilon = 0.06$, $\gamma = 1200$: (– – –) fixed boundary model; (—) undetermined boundary model; and (···) trivial equilibrium model.

increases. This is because the steady-state curvature induced from bending stiffness decreases with increasing pulley radius.

When $R/L \gg 1$ (although physically we have the limitation $R/L < 1/2$ unless the pulleys are misaligned), the natural frequencies of the fixed boundary model converge to those of the trivial equilibrium case, but those of the undetermined boundary model converge to a lower value. To examine this, note that the deflection and curvature of the beam are small for $R/L \gg 1$ or small

bending stiffness $\varepsilon \ll 1$. Under either of these conditions, the linearized equations (6) are

$$(\hat{P} - GV)' = 0, \quad (\hat{P} - GV)\kappa - \mathrm{EI}\,\kappa'' = 0. \tag{10}$$

Integrating each of these gives

$$\hat{P} - GV = \hat{P}\Big|_{s=\hat{L}/2} - GV|_{s=\hat{L}/2} = P - Gc = T, \quad T\theta - \mathrm{EI}\,\theta'' = \text{Constant}, \tag{11}$$

where P and c are the beam tension and speed at the midpoint of the free span and $\kappa = \mathrm{d}\theta/\mathrm{d}s$. For the case of two pulleys having the same radius, the slope θ and shearing force $\mathrm{EI}\,\theta''$ vanish at the midpoint, so the second of Eq. (11) gives

$$\mathrm{EI}\frac{\mathrm{d}^2\theta}{\mathrm{d}s^2} - T\theta = 0 \quad \Rightarrow \quad \theta(s) = C_1 \mathrm{e}^{\sqrt{(T/\mathrm{EI})}s} + C_2 \mathrm{e}^{-\sqrt{(T/\mathrm{EI})}s}, \tag{12}$$

where C_1 and C_2 are constants. Substitution of $\kappa(0) = \theta'(0) = -1/R$ and $\theta(\hat{L}/2) = 0$ gives

$$C_1 = \frac{(1/R)\sqrt{(\mathrm{EI}/T)}\,\mathrm{e}^{-\sqrt{(T/\mathrm{EI})}\,\hat{L}/2}}{\mathrm{e}^{\sqrt{(T/\mathrm{EI})}\,\hat{L}/2} + \mathrm{e}^{-\sqrt{(T/\mathrm{EI})}\,\hat{L}/2}}, \quad C_2 = \frac{(1/R)\sqrt{(\mathrm{EI}/T)}\,\mathrm{e}^{\sqrt{(T/\mathrm{EI})}\,\hat{L}/2}}{\mathrm{e}^{\sqrt{(T/\mathrm{EI})}\,\hat{L}/2} + \mathrm{e}^{-\sqrt{(T/\mathrm{EI})}\,\hat{L}/2}}. \tag{13}$$

Belt (and many other) applications usually have $\mathrm{EI}/T\hat{L}^2 \ll 1$, which gives $C_1 \approx 0$ and $C_2 \approx (1/R)\sqrt{(T/\mathrm{EI})}$. In Eq. (12) letting $s = 0$ gives

$$\theta(0) \approx \frac{1}{R}\sqrt{\frac{\mathrm{EI}}{T}} \tag{14}$$

Although the derivation procedure is somewhat different, the result (14) is similar to that derived by Gerbert [15] except that in Gerbert's case T represents the tension at the span midpoint. The difference is because Gerbert neglects beam inertia.

The length of the free span is increased by approximately $2R\theta(0) = 2\sqrt{\mathrm{EI}/T}$, which is the length difference between these two models as the free span end segments unwrap from the pulleys beyond the points on the common tangent line (Fig. 1(b)). This increased length, which is independent of R and L, causes the natural frequencies of the undetermined boundary model to converge to a lower value than the other two models (Fig. 6).

Notice that the above derivation and the conclusion (14) also apply to the case of small bending stiffness ($\varepsilon \ll 1$) with finite end pulley radii because Eq. (10) only requires small deflection and curvature. For such cases, the free span length is increased by $2\sqrt{\mathrm{EI}/T}$.

5. Summary

For the free vibration of axially moving beams, two different models considering the bending effect of the beam wrapping around the bounding pulleys are discussed. The commonly used model having a trivial equilibrium independent of pulley wrapping is also compared.

Bending of the moving beam around the bounding pulleys causes a non-trivial steady motion about which the system vibrates. This steady curvature tends to increase the beam natural frequencies. The fixed boundary model (Fig. 1(a)) overestimates the natural frequencies due to the underestimated span length, especially for large bending stiffness. For the undetermined

boundary model (Fig. 1(b)), as bending stiffness increases, some natural frequencies initially decrease when the bending stiffness is small because the dominant effect of bending stiffness increased free span length in this range.

Unlike the trivial equilibrium model, natural frequencies do not decrease monotonically with beam axial speed for both of the non-trivial steady-state models because increasing beam speed increases curvature in the steady state. For the fixed boundary model, increasing beam speed increases the curvature, which stiffens the system. For the undetermined boundary model in addition to increasing the curvature, increasing beam speed increases the free span length, which softens the system.

Acknowledgment

The authors thank Mark IV Automotive/Dayco Corporation and the National Science Foundation for support of this research.

References

[1] R.S. Beikmann, Static and Dynamic Behavior of Serpentine Belt Drive Systems: Theory and Experiments, PhD Dissertation, University of Michigan, Ann Arbor, MI, 1992.
[2] S.J. Hwang, N.C. Perkins, Supercritical stability of an axially moving beam Part I: model and equilibrium analysis, *Journal of Sound and Vibration* 154 (1992) 381–396.
[3] S.J. Hwang, N.C. Perkins, Supercritical stability of an axially moving beam Part II: vibration and stability analysis, *Journal of Sound and Vibration* 154 (1992) 397–406.
[4] L. Kong, R.G. Parker, Equilibrium and belt-pulley vibration coupling in serpentine belt drives, *Journal of Applied Mechanics* 70 (2003) 739–750.
[5] L. Kong, R.G. Parker, Steady state mechanics of belt-pulley systems, *Journal of Applied Mechanics*, in press.
[6] L. Kong, R.G. Parker, Coupled belt-pulley vibration in serpentine drives with belt bending stiffness, *Journal of Applied Mechanics* 71 (2004) 109–119.
[7] C.D. Mote Jr., W.Z. Wu, Vibration coupling in continuous belt and band systems, *Journal of Sound and Vibration* 102 (1985) 1–9.
[8] K.W. Wang, C.D. Mote Jr., Vibration coupling analysis of band/wheel mechanical systems, *Journal of Sound and Vibration* 109 (1986) 237–258.
[9] P.F. Turnbull, N.C. Perkins, W.W. Schultz, Contact-induced nonlinearity in oscillating belts and webs, *Journal of Vibration and Control* 1 (1995) 459–479.
[10] J.A. Wickert, Non-linear vibration of a traveling tensioned beam, *International Journal of Non-Linear Mechanics* 27 (1992) 503–517.
[11] M. J. Leamy, On a new perturbation method for the analysis of unsteady belt-drive operation, *Journal of Applied Mechanics*, submitted for publication.
[12] S.E. Bechtel, S. Vohra, K.I. Jacob, C.D. Carlson, The stretching and slipping of belts and fibers on pulleys, *Journal of Applied Mechanics* 67 (2000) 197–206.
[13] M.B. Rubin, An exact solution for steady motion of an extensible belt in multipulley belt drive systems, *Journal of Mechanical Design* 122 (2000) 311–316.
[14] N.C. Perkins, C.D. Mote Jr., Comments on curve veering in Eigenvalue problems, *Journal of Sound and Vibration* 106 (1986) 451–463.
[15] G. Gerbert, *Traction Belt Mechanics*, Chalmers University of Technology, Sweden, 1999.